This document is the accepted manuscript version of the following article:
Treydte, K., Lehmann, M. M., Wyczesany, T., & Pfautsch, S. (2021). Radial and axial water movement in adult trees recorded by stable isotope tracing. Tree Physiology. https://doi.org/10.1093/treephys/tpab080

Radial and axial water movement in adult trees recorded by stable isotope tracing

Running title:

Radial and axial water movement in trees

Kerstin Treydte[1*], Marco M. Lehmann[1], Tomasz Wyszesany[2], Sebastian Pfautsch[3,4]

[1] *Research Unit Forest Dynamics, Swiss Federal Institute for Forest, Snow, and Landscape Research WSL, Birmensdorf, Switzerland*

[2] *Plant Functional Biology and Climate Change Cluster, University of Technology, Sydney, Australia*

[3] *Hawkesbury Institute for the Environment, University of Western Sydney, Richmond, Australia*

[4] *Urban Studies, School of Social Sciences, Western Sydney University, Parramatta, Australia*

***Corresponding Author**

Kerstin Treydte

Email: kerstin.treydte@wsl.ch

Tel: +41 44 739 2662

Key words: labelling experiment; heavy water; tree water relations; Eucalyptus; sapflow

Abstract

The capacity of trees to release water from storage compartments into the transpiration stream can mitigate damage to hydraulic functioning. However, the location of these 'transient' water sources, and also the pathways of water movement other than vertical through tree stems still remains poorly understood. We conducted an experiment on two tree species in a common garden in eastern Australia that naturally grow in regions of high (*Eucalyptus tereticornis*, 'Red Gum') and low (*Eucalyptus sideroxylon*, 'Ironbark') annual precipitation rates. Deuterium enriched water (1350 ‰ label strength) was directly introduced into the transpiration stream of three trees per species for four consecutive days. Subsequently the trees were felled, woody tissue samples were collected from different heights and azimuthal positions of the stems, and stable isotope ratios were determined on the water extracted from all samples. The presence/absence of the tracer along the radial and vertical stem axes in combination with xylem hydraulic properties inferred from sapflow, leaf and stem water

potentials, wood moisture contents and anatomical sapwood characteristics elucidated species-specific patterns of short-term stem water storage and movement. The distribution of water isotopes at natural abundance among woody tissues indicated systematic differences with highest values of sapwood water and lower values in inner bark and heartwood. Presence of tracer in water of the inner bark highlighted the importance of this tissue as capacitor. While injected at the northern side of stems, tracer was also discovered at the southern side, providing empirical evidence for circumferential flow in sapwood, particularly of Ironbark. Greater vertical water transport in Red Gum compared to more radial and circumferential water transport in Ironbark were associated with species-specific sapwood anatomy. Our study highlights the value of combining information from stable isotope tracers and wood anatomy to investigate patterns of water transport and storage of tall trees *in situ*.

Introduction

A key role for the ability of trees to endure drought and heat related climatic extremes is their capacity to release water from storage compartments into the transpiration stream to mitigate damage to hydraulic functioning (Wullschleger et al. 1996; Borchert and Pockmann 2005; Meinzer et al. 2006; Pfautsch et al. 2013, 2016; Matheny et al. 2015). Various studies have demonstrated that 10–50% of daily transpiration may be provided by water stored in stem tissues (Waring and Running 1978; Goldstein et al. 1998; Phillips et al. 2003; Cermak et al. 2007; Kocher et al. 2013; Matheny et al. 2015). Even in case the absolute amount of water obtained from internal storage during a day may be relatively small, its role in the maintenance of favorable leaf water potential and carbon balance may nevertheless still be significant (Logullo and Salleo 1992; Goldstein et al. 1998).

While our knowledge on theoretical functioning of the processes of stem water storage and its mobilisation is improving (Huang et al. 2017), we still lack empirical evidence of these

functions, and the location and dynamics of these 'transient' internal water sources still remains poorly defined. This is particularly the case for large trees growing under natural conditions, since many experimental studies are limited to small, potted trees grown in controlled environments. Besides, most of the growing literature on water movement in intact trees has emphasized the use of sap flow techniques to estimate whole-tree water use, however, a number of uncertainties in processing of relevant data remain (Peters et al. 2018). *In situ* observations of storage and movement are still rare, and existing experimental studies focussed on short-distance transfer of water or minerals injecting dyes such as fluorescent tracers (Sano et al. 2005; Sokołowska 2012; Pfautsch et al. 2015a), caesium (Kuroda et al. 2018) or rubidium and europium (Okada et al. 2011). Those studies particularly emphasize the role of radially aligned and interconnected ray parenchyma cells as transport pathways that functionally link the tissues of the inner bark and xylem (Pfautsch et al. 2015b).

Stable isotopes of hydrogen and oxygen ($\delta^{2}H$ and $\delta^{18}O$) in water and organic materials are a valuable tool in ecological, biogeochemical, hydrological and paleoclimate research and have been used as hydrological and ecophysiological tracers for more than five decades (Kendall and McDonnell 1998; Dawson et al. 2002; Vitvar et al. 2005; Werner et al. 2012; Penna et al. 2018). Isotope tracers, such as water enriched in the heavy isotopes ^{2}H and ^{18}O, have successfully been used to characterize the relationship between tree hydraulic architecture and whole-tree water flux, storage and retention of water in plants (James et al. 2003; Meinzer et al. 2006; Zapater et al. 2011; Rothfuss and Javaux 2017; Lehmann et al. 2018; Penna et al. 2018; Wang et al. 2020). However, most of these studies were restricted to young trees grown under controlled greenhouse conditions, single larger trees, or as 'proof of concept' that injected ^{2}H (also known as Deuterium, abbreviated 'D') and ^{18}O can be used to trace transpiration water. Information about the distribution of water isotopes at natural abundance among different woody tissues along adult tree stems and potential differences in there is,

however, still scarce. Yet, such information would provide valuable insight into potential short-term shifts in soil water uptake, and water retention in these tissues. And even more, no study has yet documented the movement of an isotope tracer along the entire stem of tall trees, including in radial and circumferential direction and between inner bark, sapwood and heartwood.

Here we conducted a labelling experiment with deuterium enriched 'heavy water' (D_2O) to investigate the radial and vertical water movement in and short-term water storage of adult trees. For this purpouse we selected two tree species typical for Australia, grown next to each other in a common garden: *Eucalyptus tereticornis*, a species fround in mesic coastal regions and *Eucalyptus sideroxylon*, which copes well with more xeric inland conditions. As shown previously, sapwood traits in eucalypt species tend to reflect long-term genetic adaptation, rather than short-term environmental variability (Pfautsch et al. 2016). It was thus expected that the two species retained large differences in sapwood traits even though they were grown for more than a decade under the same environmental conditions. Further support for this assumption was drawn from the observation that Red Gum trees had nearly twice the height and stem diameter of Ironbark (Fig. 1), representing an ideal setting to comparatively study species differences in patterns of water movement *in situ* and corresponding sapwood traits (James et al. 2003). We hypothesized that both tree species differ i) in the stem water storage characteristics of their tree tissues, ii) in their radial and axial stem water movement patterns, and iii) that these differences are related to their different xylem (i.e. sapwood and heartwood) hydraulic properties. To test these hypotheses, we used stable isotope tracing in combination with the distribution of water isotopes at natural abundance to characterize patterns of water storage and movement i) between inner bark, sapwood and heartwood, ii) along the vertical stem axes and circumferential direction, and iii) to compare these patterns with xylem

hydraulic properties inferred from sapflow, leaf water potential, wood moisture content, and, most importantly, vessel anatomical characteristics.

Material and Methods

Study site and trees

The study was conducted in a 15-year old common garden planting at the Hawkesbury Forest Experiment site in Richmond, 60 km northwest of Sydney, Australia (25 m above sea level; 33° 369 4099 S, 150° 449 26.599 E) using two eucalypt species (Fig. 1). *Eucalyptus tereticornis* (in the following 'Red Gum') is one of the most widespread eucalypts in Australia, distributed along the eastern seaboard from southern Victoria to northern Queensland. It grows at locations where mean annual precipitation is > 600 mm. *Eucalyptus sideroxylon* (in the following 'Ironbark') occurs further inland in south-eastern Australia at locations with mean annual precipitation > 400 mm. It is known to be slower growing and more drought tolerant than Red Gum (Drake et al. 2017; Duan et al. 2018).

Climate at the study site is warm-temperate: Mean annual temperatures reach 17.7 °C, with January as the warmest (24.0 °C) and July as the coldest month (10.6 °C). Annual precipitation averages 728 mm, with a maximum in summer (114.0 mm in February), and a minimum in winter (27.5 mm in July) (long-term means of the period 1993-2018 for Richmond NSW; Bureau of Meteorology, Australian Government).

The common garden was arranged as randomised block design, with 12 gymnosperm and angiosperm species in 6 replicate blocks. We selected three trees per species for the trace labelling experiment ('experimental trees') and one tree per species without tracer as control ('control tree') from within a single block to minimise potential differences in access to soil nutrients and water. Selected Red Gum individuals were between 17 and 23 m tall and stem

diameters at 1.3 m above the ground ranged from 17.5 to 31.6 cm. Height of selected Ironbark trees was between 9.5 and 12.5 m and stem diameters between 15.7 and 20.8 cm.

The experiment was split into two periods: During the first period (March 13-16, 2014) we examined Red Gum and during the second period (March 20-23, 2014) we examined Ironbark. Weather conditions during both periods were similar, with typical diurnal patterns of photosynthetic active radiation and VPD, reaching their minima at late night and maxima around noon. A small thunderstorm occurred in the morning of 16 March and the evening of 21 March (Fig. 2a). Meteorological data such as mean, maximum and minimum temperatures, rainfall, relative humidity and solar radiation values measured in 15-minutes intervals were available from a nearby climate station at the Hawkesbury Forest Experiment site of which the common garden was part. Vapour pressure deficit (VPD in kPa) was calculated using air temperature and relative humidity according to Snyder and Shaw (1984).

Injection of deuterium enriched water into the tree stems

Devices for injection of heavy water (D_2O) were installed at about 1 m stem height on the northern (N), sun exposed side of each stem. A PVC connector (45° cut angle, 100 mm long, 50 mm wide) was mounted onto the tree stem using a steel bracket and screws (35 mm long). A water-tight seal between the exposed sapwood and the PVC connector was produced using a 2-component marine epoxy putty. Once the seal had hardened, the connector was filled with water and a 5 mm diameter injection hole was carefully drilled about 30 mm deep into the sapwood (Table 2) at a downward 45° angle. Drilling was done with a cordless drill and a specialized long drill bit (5 mm diameter, 300 mm length) to produce a clean-cut insertion hole. All drilling was undertaken before or around noon and under water to avoid entry of air into conducting sapwood vessels. While still some cavitation could have occurred due to the

Wheeler effect (Wheeler et al. 2013), possibly cavitated conduits should have refilled after, due to the small positive pressure created during water injection.

Drilled holes were flushed with MilliQ water to displace any wood debris. Bespoke water reservoirs made from PVC pipes (ca. 500 mm long, 50 mm wide) were mounted onto the connector (Fig. 1), and carefully filled with about one liter of D_2O ('heavy water') with a label strength of 1350 ‰ and a $\delta^{18}O$ value of -3.43 ‰ and refilled periodically as the D_2O was taken up into the transpiration stream. After each refilling the reservoirs were closed with a lid to avoid evaporative enrichment or mixing with atmospheric moisture. The lid was fitted with a 20 cm long and 2 mm wide plastic tubing to allow equilibration of air pressure inside the reservoirs with ambient conditions. The reservoirs remained affixed to stems for four consecutive days.

Tree water use

Water use of the experimental trees was monitored prior and during D_2O injection using heat ratio probes (HRM30, ICT International, Armidale, Australia; see Burgess et al., 2001 for theory of the method). Probes were installed above the reservoir at the northern and in addition also at the southern side of each stem. Sap velocity was recorded simultaneously at two depths every 15 minutes and transformed to sap flow use as described in Pfautsch et al. (2010). Sap flow density (Q_s) was calculated on a unit sapwood area basis. Cumulative water use was calculated by summing up sap flows for both depths over one hour and dividing this sum by four, before converting to litres. The total sapwood area was estimated from stem disks extracted from felled trees and divided in equal proportions to differentiate between water moving upwards at the northern and southern side of the trees (Table 2).

Leaf water potential and tissue moisture

Pre-dawn and midday leaf water potentials on five leaves from each experimental tree were measured with a Scholander-type pressure chamber (1505D-EXP; PMS Instrument Company, OR, United States) on 13th and 20th of March (hereafter termed 'day one'). On each day prior to pre-dawn leaf collections, three leaves of each experimental tree were wrapped in aluminium foil and enclosed in a ziplock bag. These leaves were collected during midday and represented a proxy for stem water potential. All leaf collections were conducted using a a hydraulic platform for access. Moisture content in inner bark, sap- and heartwood were also measured once during daytime on day one using samples from three additional trees per species. For this purpose, increment cores (5 mm diameter) were extracted at 1.3 m above ground, tissues were separated (clear color change between sapwood and heartwood in both species), and their fresh weight noted. After drying these tissues at 105 °C for 48 hours to constant weight, their dry weight was noted, and tissue moisture content calculated as difference between fresh and dry weights in percent: $\%\ moisture = \frac{fresh\ weight - dry\ weight}{freshweight * 100}$

Sampling of tree tissues, water extraction and water isotope measurements

After feeding D_2O for four consecutive days into the base of the stems, experimental trees and the control tree were felled. Samples of woody tissues, i.e. inner bark (outer dead bark was discarded), sapwood and heartwood were taken from four heights (Fig. 1; above the reservoir ('low'), at 33% ('mid') and 66% ('up') of the total tree height and at the very top ('apex')). Heartwood samples were taken at the approximate mid-point between the sapwood-heartwood boundary and the pith. All samples except the 'apex' were taken at the northern as well as at the southern side of the stems. In addition, a few samples were taken right below the feeder on the northern side of the stems ('base'). Sampling was conducted with a chain saw to extract whole wood discs and subsequent use of a hammer and a chisel (stem samples),

or a pruner (apex samples) to generate manageable sample sizes. All tools used during the felling and sample collection were carefully cleaned with de-ionized water after each step to avoid cross-contamination of samples. Samples were collected in duplicate at each position to provide materials for sapwood anatomical analyses and extraction of tissue moisture. It has to be noted, that in seven out of eight trees heartwood was only present at the low and mid sampling position of the stems and absent higher up. Immediately after extraction, samples were transferred to airtight containers and stored on ice until further lab procedures. A total of 168 tissue samples were collected.

Water extraction of all woody samples was done by cryogenic vacuum extraction at UTS (Orlowski et al. 2013; Newberry et al. 2017) and hydrogen and oxygen isotope measurements were conducted with a Picarro laser (L2132-i, Picarro Inc., Santa Clata, USA) with a measurement precision (one standard deviation, SD) of ±1‰ for δ^2H and ±0.3 ‰ for $\delta^{18}O$. All isotope values were normalized to VSMOW (Vienna Standard Mean Ocean Water). Measurements were checked with the ChemCorrect software to identify potential errors introduced due to spectral interference with organics (Gerlein-Safdi et al. 2017). Only 14 samples our of 168 were flagged, but no systematic bias towards specific sample types such as bark was found. This is in line e.g. with Carrière et al. (2020) who reported no difference between plant xylem water δ^2H measurements conducted with laser spectroscopy and IRMS and with Volkmann et al. (2016) who confirmed no contamination by organics during in-situ online xylem water δ^2H measurements using laser spectroscopy.

Wood anatomical measurements

Sapwood vessel traits in 56 sapwood samples were assessed using optical microscopy. Cross sections (25 μm thickness) of sapwood were prepared using a sliding microtome (Leica

RM2255; Leica Microsystems, Wetzlar, Germany). Tissue sections were stained with safranin (1% aqueous) and washed clean before wet-embedding them on a glass slide and cover glass. Six digital images were taken of each section at 40X (stem samples) and 200X (apex samples) using a transmission light microscope (Leica SM2010 R; Leica Microsystems) equipped with a digital camera (Leica DFC 500; Leica Microsystems). Wood anatomical characteristics were measured by image analysis (ImageJ, National Institutes of Health, Bathesda, USA). Altogether 8456 vessels were analysed. Investigated traits were: (i) sapwood vessel diameter, (ii) hydraulically weighted vessel diameter, (iii) vessel frequency and (iv) the void/wood ratio. For scanning electron microscopy, wood samples were cut into approximately 8 to 10 mm cubes, and all sides were trimmed using a microtome to provide clean and smooth surfaces (Pfautsch et al. 2015a). Sample blocks were mounted on aluminum stubs with double-sided carbon adhesive tape, allowing imaging of transverse planes. A scanning electron microscope (6510LV; JEOL) operated in low-vacuum mode at a vacuum chamber pressure of 50 Pa, 20kV accelerating voltage, and 15mm working distance. The resulting images were used to determine species- and location-specific differences in ray parenchyma traits (i.e. arrangement and number of rays in files).

Data analysis

The non-parametric Kruskall-Wallis test and a post-hoc pairwise Wilkoxon rank sum test without continuity correction were used for testing the significance of differences between independent groups of data with unequal variance (holds for all types of data used here) and partly non-normal distributed data (holds fr δ^2H data of the treated trees). Homogeneity of variance between groups was assessed with the Bartlett test and (non-)normal distribution of data was identified using the Shapiro normality test.

The presence or absence of the deuterium tracer in a sample of the different tree tissues was identified by calculating the δ^2H difference ($\Delta\delta^2H$) between experimental and control trees. Positive $\Delta\delta^2H$ deviations indicate presence of the tracer and negative $\Delta\delta^2H$ deviations indicate its absence. A one sample t-test was applied to test the significance of the differences between the means of the treated trees and the δ^2H value of the corresponding water sample of the control. Linear regression analysis was applied to test for statistic relationships between δ^2H and $\delta^{18}O$ data of the control trees, but further investigation of the experimental trees was based on δ^2H only. For all tests, differences were considered significant at $p<0.05$. Staistical analyses were performed in R, version 4.0.3 (R Core Team 2020; RStudio Team 2020). Graphs were plotted with the R package 'ggplot2' (Wickham 2016).

Results

Sapflow, leaf water potentials and wood moisture content

Patterns of sap flow through all trees followed a typical diurnal cycle with a pronounced increase of flow around sunrise, peak flow when VPD and hence transpiration was high, a decrease in flow during the afternoon and close-to-zero flow during the night (Fig. 2). The larger sap flow on the northern side of four out of six trees (except Ironbark tree number 1 and 3) was the result of larger sapwood area on that side of the stems.

Importantly, the sap flow data showed that drilling into the sapwood and installation of the reservoirs did not affect water transport patterns and volumes, since the pattern of Q_s remained unchanged between the northern and southern sides of the stems. Only in one Red Gum tree (tree number 1; Fig. 2) the water flux decreased during the four days of the experiment, because the reservoir of this tree accidentally emptied completely, which likely caused blockage of some sapwood vessels at this side of the tree. Nevertheless, transport of

the deuterium tracer was still strong enough to generate distinct isotope signals (i.e. maximum $\Delta\delta^2H$ values in Fig. 8 in sapwood water at the northern up and apex positions, and bark water at the apex are from this tree). The average daily water transport in Ironbark was half the amount (15 L d^{-1}) of that observed in Red Gum (30 L d^{-1}) (Fig. 3). Since VPD and solar radiation values were in a similar range during the two study periods (Fig. 2), the difference in water transport seems to be species-specific.

Both species showed high leaf water potentials at pre-dawn and low leaf water potentials at midday. In Ironbark leaf and also stem water potentials at both times of the day were significantly ($p<0.01$) lower (mean predawn LWP: -0.84 MPa, mean midday LWP: -1.82 MPa) compared to Red Gum (mean predawn LWP: -0.43 MPa, mean midday LWP: -1.24 MPa) (Fig. 4).

Moisture contents (Table 1) of both inner bark and heartwood from Red Gum were significantly larger ($p<0.05$) than of those from Ironbark with a difference of 12 % and 15 % respectively. Also, sapwood moisture was lower at least for two out of three Ironbark trees compared to Red Gum. The highest moisture content was recorded in the inner bark of both species (Red Gum: 62 %; Ironbark: 50%), followed by heartwood (52 %) and sapwood in Red Gum, while in Ironbark heartwood had the lowest moisture content of all three tissues (37 %) (Table 1). In both species, differences between the moisture content of the three tissues were, however, not statistically significant ($p>0.05$).

Sapwood anatomy

Analyses of sapwood traits revealed that compared to Red Gum, Ironbark had denser sapwood, narrower yet more frequent vessels and a slightly lower void/wood ratio (Table 3). This applies to all positions within stems, including the apex. In Ironbark the sapwood density tended to slightly decrease with stem height, and this also holds for the maximum and

hydraulically weighted vessel diameter, while the minimum vessel diameter remained stable. The void/wood ratio of both species also slightly increased with stem height.

Furthermore, the analysis of the tangential sections (Fig. 5) revealed marked differences in the abundance and organisation of ray parenchyma. Whereas rays were organised exclusively in monoseriate files in Red Gum, mono- and biseriate files were present in sapwood of Ironbark. The latter species also exhibited a larger total number of individual rays at any position along the stem (Table 4).

Tissue water δ^2H and $\delta^{18}O$ patterns at natural abundance

Overall, no significant species-specific differences were found between the water isotope data sets of the two control trees, though δ^2H values of Ironbark tended to be slightly lower compared to Red Gum (Fig. 6a, Table S1). Correlations between δ^2H and $\delta^{18}O$ values were highly significant ($p<0.001$) for both control trees (Figure 6a) in general and also, more specifically, for sapwood and inner bark water ($p<0.01$) (Fig. 6b). Mean sapwood water isotope values were significantly higher compared to inner bark and heartwood water ($p<0.05$) (Fig. 6b, Table S1).

Along the vertical stem axes (Fig. 7; Fig. S1), particularly inner bark water isotope values decreased towards a minimum at the apex. Sapwood water isotopic signatures at the base and low sampling positions of both tree stems were higher compared to the other sampling positions, but remained fairly stable at the mid, up and apex sampling positions. Heartwood water δ^2H values increased from the low to the mid sampling positions (with the only exception at the northern side of the Ironbark tree) (Fig. 7; Fig. S1). Isotope values of the northern and southern side of the tree stem water were fairly similar among species, tissues and stem heights (Fig. 7). Only inner bark water δ^2H values at the mid and upper positions of

the Ironbark stem were higher at the northern side (Fig. 7c and d). Particularly systematic differences between the woody tissues from one single tree per species are well supported by the distribution of $\delta^{18}O$ signatures in the experimental trees, which were seen to not be affected by the deuterium tracer (Fig. S2; Table S1).

Identification of the deuterium tracer along the radial and vertical stem axes

Deuterium labelled water could be identified in most of the samples of the treated trees (Fig. 8), although variations among individual trees and tissues were in some cases large. With a mean positive deviation ($\Delta\delta^2H$) of 380 ‰ (max 675.12 ‰) from the corresponding sample of the control, the tracer was most prominent in sapwood just above the reservoir (low position) in both species. Positive deviations of the other samples ranged between 5 to 35 ‰.

In the experimental Red Gum trees significant differences ($p<0.01$) were found between the northern and southern side of the stems with greater mean ^2H enrichment of both sapwood and bark water at the northern side (Fig. 8a and b). There, mean sapwood water $\Delta\delta^2H$ values increased from 31.02 ‰ at mid to 41.52 ‰ at up and decreased to 26.21 ‰ at the apex positions while mean values varied around 10 ‰ at the southern side. Mean inner bark water $\Delta\delta^2H$ values at the northern side increased from 27.44 ‰ at the low sampling positions to 37.38 ‰ (mid) and 37.74 ‰ at the up positions, before strongly decreasing at the apex (13.55 ‰). At the southern side, however, the presence of the tracer was sporadic at best. Heartwood water at the northern side was only slightly ^2H enriched compared to the control and the tracer was completely absent at the southern side of the trees stems.

A different $\Delta\delta^2H$ pattern was found in Ironbark trees (Fig. 8c and d) with clear presence of the tracer at both sides of the stems (differences non-significant), in all of the three tree tissues and at all sampling heights. Mean sapwood values at the northern side of the stems varied

between 23.0 ‰ at mid, 20.9 ‰ at up and 18.06 ‰ at apex positions. At the corresponding sampling positions of the southern side values declined from 28.0 ‰ to 18.4 ‰ and 18.1 ‰. In inner bark water, $\Delta\delta^2H$ values declined from 23.2 ‰ to 23.7 ‰ and 20.6 ‰ at the northern side of the stems and from 30.2 ‰ to 22.6 ‰ and 20.6 ‰ at the southern side. Also all but one heartwood sample had positive $\Delta\delta^2H$ values.

Discussion

Radial and vertical distribution of water isotopes at natural abundance

In general, the distribution of water δ^2H and $\delta^{18}O$ values of the tree tissues and particularly of the sapwood at natural abundance are in the range of the isotopic signatures of precipitation water in the region. Those have been reported to vary from the East coast to the Blue Mountains on average between -22.6 and -32.6 ‰ for δ^2H and between -4.8 and -6.2 ‰ for $\delta^{18}O$ (annual average for the period 2005-2008) (Hughes and Crawford 2013), but with huge seasonal and inter-annual variability. Overall slightly ^{18}O- and ^2H depleted water in *Ironbark* compared to *Red Gum* could either be related to water uptake of *Ironbark* from deeper soil layers, or because of a longer residence time of water in the stem and protection against evaporation by its thick bark.

We found systematic differences in the isotope signatures of the different woody tissues and partly also along the vertical tree axes. Isotope values in inner bark water were depleted compared to those of sapwood and heartwood water, and a distinct decrease was found towards the apex. This finding contradicts other studies that report bark water to be rather enriched in ^2H and ^{18}O compared to sapwood and - particularly in the upper part of the trees - being close to the signature of the generally enriched leaf water (Thorburn et al. 1993; Cernusak et al. 2005, 2016; Gessler et al. 2014). No systematic inference with organics

ocured during the laser spectroscopy measurements (see Methods), but still some extracted bark sap may have contained volatile organic compounds For Ironbark it has beeen recently reported by Ferreira et al. (2018) that these can be strongly depleted in ^{2}H. Though somehow speculative, progressive depletion of inner bark water along the vertical axis could also be caused by a sustained imbalance against deuterium in the water exchange between the transpiration stream and inner bark cells due to surface isotopic effects (Chen et al. 2016; Zhao et al. 2016; Barbeta et al. 2020).

Fairly stable sapwood water isotope values along the mid, up and apex positions suggest a consistently close link to a relatively stable soil water source and only minor fractionation effects during root water uptake and water transport through the sapwood to the evaporative sites (e.g., leaves and non-lignified green branches) (Wershaw et al. 1966; White et al. 1985; Walker & Richardson 1991; Dawson & Ehleringer 1993; Dawson et al. 2002; Zhao et al. 2016). We assume that our study trees had access to a continuous, probably relatively deep and stable soil water reservoir due to their extended root system and, hence, did not face major diurnal variations in the soil moisture gradient as has been reported recently (De Deurwärder et al. 2020). Strong enrichment of sapwood and heartwood water samples from the base and low positions compared to the other positions of the control trees was most probably an artefact caused by evaporation due to a delay in the sampling procedure at these individuals after tree felling.

Our finding of depleted water in heartwood compared to the other tree tissues is in line with the few studies that also tested the distribution of water isotopes in woody tissues at natural abundance separately: White et al. (1985) found significantly depleted $\delta^{2}H$ values in trunk heartwood water compared to sapwood of *Taxodium distichum* at three sites over a 3-week period. They attributed the difference to a lack of equilibrium between the two parts of the trunk in response to variations in sapwood $\delta^{2}H$ as the tree obtained water from isotopically

different sources (soil and groundwater). Thorburn et al. (1993) reported lower values of heartwood water from two Eucalypt species (*E. oleosa* and *E. gracilis*) compared to sapwood water, but only for one of two investigated sampling dates and at one of two sites. They also explain the difference by a shift in the water source from soil to groundwater.

Stem water movement recorded by D_2O tracing in relation to hydraulic architecture

The trace labelling experiment was successful for the qualitative assessment of vertical, but even more interestingly, also for radial (i.e. inner bark, sapwood, heartwood) and circumferential (i.e. northern *vs* southern side of the stems) movement of water within the tree stems, and revealed systematic differences between both species in relation to their hydraulic architecture.

In Red Gum the distribution of the tracer suggested predominantly vertical movement of water within the transpiration stream of the sapwood: It was present in sapwood at all sampling positions at the northern side of the stems where water injection took place, but very low (sapwood and inner bark) or no (heartwood) enrichment was found at the opposite sides of the stems. Inner bark water was markedly enriched indicating a distinct radial movement of the tracer to the outside of the stems. No clear dispersion into the heartwood was, however, detected since the tracer was only present in the samples close to the water injection at the low, and less at the mid sampling position at the northern side of the stems, and it was fully absent at the opposite sides of the stems. Along the northern vertical stem axes enrichment of sapwood and inner bark water indicated efficient water uptake. This finding contradicts our expectation that the tracer signal may have been diluted in Red Gum compared to Ironbark due to a higher water content and a larger amount of water transported.

In Ironbark the distribution of the tracer suggested a distinct radial and circumferential movement of water between tree tissues and along the stem axes. Tracer was not only present

in inner bark and sapwood, but also in heartwood, and transferred from the side of water injection to the opposite side of the stems, and also into all three stem tissues there. Further, the strength of enrichment of sapwood and inner bark water decreased along the vertical stem axes, also supporting the hypothesis of distinct radial and circumferential water movement.

These species-specific patterns of water movement are in close relation to the hydraulic architecture of both tree species. Compared to Red Gum, Ironbark had lower leaf water potentials, higher sapwood density, a lower total and hydraulically weighted vessel diameter, a higher density of the vessels and a slightly lower void/wood ratio. All these traits indicated less overall space to be attributed to conduct water and a higher soil-to-leaf hydraulic resistance.

Moreover, the central role of radially aligned and interconnected parenchyma cells in linking the tissues of the inner bark region (i.e. phloem) and the xylem (both sapwood and heartwood) and their capability of symplastic water transport has been frequently stressed (Zweifel et al. 2001; Sevanto et al. 2011; Pfautsch et al. 2015a,b). Radial transfer of water is known to be a function of differences in water potential between xylem and inner bark and radial hydraulic conductivity (Pfautsch 2015). A larger number of parenchyma rays, more intersections (pits) between vessels and rays, and biseriate rays in Ironbark increase its capacity for radial and circumferential water transport and enhance the bidirectional flow between phloem and xylem compared to Red Gum. While in heartwood tyloses will have blocked vertical transport of water in the vessels, particularly axial parenchyma cells may nevertheless at least partly remain open (Chattaway 1949) and connected with the sapwood, which would explain the movement of tracer into the heartwood at the mid positions of both sides of the stems.

Active radial transfer of water from outer to inner sapwood and even into heartwood through ray parenchyma of *Cryptomeria japonica* trees has been reported by Okada et al. (2011, 2012)

in the vapour phase, applying rubidium as a tracer. Investigating water accumulation in heartwood of conifers, Nakada et al. (2019) recently confirmed the presence of a water potential gradient as possible driving factor of water movement from sapwood to heartwood and during a limited season. Our findings of not only mono- but rather bidirectional flow of water between phloem and xylem provide independent confirmation to previous studies who recorded similar transport patterns based on fluorescent tracers (Sokolowska and Zagórska-Marek 2012; Pfautsch et al. 2015a), with the extent and direction of radial transfer depending on the water potential gradient between phloem and xylem (Pfautsch et al. 2015b).

Water storage function of stem tissues

Our trace labelling study does not only demonstrate radial and axial movement of water in tree stems but even more highlights the capacitive function of stem tissues and especially of bark as the prime candidate for water storage in eucalypt trees. The transfer of water from phloem into xylem is important to mitigate increasing hydraulic tension in the vascular system during the diurnal cycle of transpiration. Up to now there exists, however, only limited direct evidence of such water transfer and the contributing pathways (Pfautsch et al. 2015a; 2016).

The capacity to store and release water depends on capillary pore spaces, free apoplastic water, the elasticity of the storage tissue, its connectivity to xylem vessels, the gradient of water potential between the storage tissue and vessels, and also cavitation (Knipfer et al. 2019). Cells with elastic walls represent ideal capacitors because they can change their volume as a consequence of small changes in water potential. Thus, phloem, cambium, and juvenile sapwood cells are well suited for water storage and release into the xylem conduits to support transpiration demand (Goldstein et al. 1998; Morris et al. 2016) or repair embolism (Secchi et al. 2017; Klein et al. 2018; Konrad et al. 2019; Knipfer et al. 2019). Particularly the

role of phloem tissue as a dynamic capacitor for water storage and transfer and its contribution toward the maintenance of the functional integrity of xylem in trees has been emphasized earlier (Pfautsch et al. 2015b). While phloem has substantial elastic storage capacity, diurnal cycles of storage in sapwood and heartwood also rely on free water in apoplastic space as well as capillary pore spaces filling and emptying (Knipfer et al. 2019). Given the continued sapflow of trees after creation of the injection hole, high negative pressure probably remained throughout the water transport system in sapwood, exerting negative pressure on water stores, even including the heartwood in case of Ironbark. High water content in heartwood as shown here but also for other eucalypt species (Pfautsch et al. 2012) makes it likely that this tissue may also serve as small reservoir in the diurnal cycle of discharge and recharge from water stores.

Overall obviously both eucalypt species studied here follow different water use strategies: Due to its vessel architecture Ironbark has a larger relative capacity to store and remobilize water in the stem compared Red Gum and, hence, is better adapted to tolerate dry conditions, mainly due to its higher resistance to cavitation during periods of water limitation. The trade-off is, however, a lower amount of water to be used even when available, and hence, slower growth rates than Red Gum (Drake et al. 2017).

Conclusion

In conclusion our study provides direct evidence for radial transfer of water between and water storage in stem tissues and, hence, supports theoretical predictions of the role of bidirectional phloem-xylem water transfer in the hydraulic functioning of trees. We particularly elucidate the strong hydraulic link between inner bark and xylem and support the currently emerging perspective of xylem and phloem as one interconnected, yet highly segregated transport network for carbohydrates and water rather than two independent

transport systems (Pfautsch et al. 2015b, 2016; Mencuccini et al. 2017; Konrad et al. 2019). We can confirm the two different strategies of the species to transport water (efficiently in Red Gum, safely in Ironbark), which allows insight into the physiological and anatomical adaptations to prevailing conditions in the home environment of the two species. An improved understanding of water storage and mobilisation in tree stems will strengthen our ability to predict the future of tree-dominated ecosystems under changing environmental conditions.

Conflict of interest

None declared.

Funding and Acknowledgements

We thank Burhan Amiji, Justine Renard, Renee Smith and Anita Wesolowsky for help in the field. We also thank Adrià Barbeta and an anonymous reviewer for valuable comments on the manuscript. Access to analytical fiacilities and technical support at the University of Technology Sydney by Derek Eamus is highly acknowledged. This work was supported by the Swiss National Science foundation (KT: IZK0Z3_154157 & 200021_175888; MML: PZ00P2_179978).

Authors' Contributions

KT and SP developed the study concept and design and conducted the experiment. KT, SP and TW collected the data. KT and SP performed the data analysis and interpretation with support by ML and TW. KT wrote the manuscript with contributions by all co-authors.

References

Barbeta A, Gimeno TE, Clavé L, Fréjaville B, Jones SP, Delvigne C, Wingate L, Ogée J (2020) An explanation for the isotopic offset between soil and stem water in a temperate tree species. New Phytologist 227: 766–779.

Borchert R, Pockman WT (2005) Water storage capacitance and xylem tension in isolated branches of temperate and tropical trees. Tree Physiology 25:457-466.

Bureao of Meteorology, Australian Government (2019) http://www.bom.gov.au/climate/ averages/tables/ cw_067105_All.shtml.

Carrière SD, Martin-StPaul NK, Cakpo CB, Patris N, Gillon M, Chalikakis K, Doussan C, Olioso A, Babic M, Jouineau A, Simioni G, Davi H (2020) Tree xylem water isotope analysis by Isotope Ratio Mass Spectrometry and laser spectrometry: A dataset to explore tree response to drought. Data in Brief 29: 105349.

Cermak J, Kucera J, Bauerle WL, Phillips N, Hinckley TM (2007) Tree water storage and its diurnal dynamics related to sap flow and changes in stem volume in old-growth Douglas-fir trees. Tree Physiology 27:181–198.

Cernusak LA, Farquhar GD, Pate JS (2005) Environmental and physiological controls over oxygen and carbon isotope composition of Tasmanian blue gum, Eucalyptus globulus. Tree Phsiology 25: 129–146.

Cernusak LA, Barbour MM, Arndt SK, Cheesman AW, English NB, Feild TS, Helliker BR, Holloway-Phillips MM, Holtum JAM, Kahmen A, McInerney FA, Munksgaard NC, Simonin KA, Song X, Stuart-Williams H, West JB, Farquhar GD (2016) Stable isotopes in leaf water of terrestrial plants. Plant, Cell & Environment 39: 1087–1102.

Chattaway M (1949) The development of tyloses and secretion of gum in heartwood formation. Australian Journal of Biological Sciences 2: 227-240.

Chen G, Auerswald K, Schnyder H (2016) 2H and 18O depletion of water close to organic surfaces. Biogeosciences 13: 3175–3186.

Dawson TE, Ehleringer JR (1993) Isotopic enrichment of water in the "woody" tissues of plants: implications for plant water source, water uptake, and other studies which use the stable isotopic composition of cellulose. Geochimica et Cosmochimica Acta 57: 3487–3492.

Dawson TE, Mambelli S, Plamboeck AH, Templer PH, Tu KP (2002) Stable Isotopes in Plant Ecology, Ann. Rev. Ecol. Syst. 33: 507–559.

De Deurwaerder H, Visser MD, Detto M, Boeckx P, Meunier F, Kuehnhammer K, Magh R-K, Marshall JD, Wang L, Zhao L, Verbeeck H (2020) Causes and consequences of pronounced variation in the isotope composition of plant xylem water. Biogeosciences 17: 4853–4870.

Drake JE, Power SA, Duursma RA, Medlyn BE, Aspinwall MJ, Choat B, Creek D, Eamus D, Maier C, Pfautsch S, Smith RA, Tjoelker MG, Tissue DT (2017) Stomatal and non-stomatal limitations of photosynthesis for four tree species under drought: A comparison of model formulations. Agricultural and Forest Meteorology 247: 454-466.

Ferreira JPA, Miranda I, Pereira H (2018) Chemical composition of lipophilic extractives from six Eucalyptus barks. Wood Science and Technology 52: 1685–1699.

Gerlein-Safdi C, Gauthier PG, Sinkler CJ, Caylor KK (2017) Leaf water ^{18}O and ^{2}H maps show directional enrichment discrepancy in *Colocasia esculenta*. Plant, Cell & Environment 40: 2095-2108.

Gessler A, Ferrio JP, Hommel R, Treydte K, Werner R, Monson RK (2014) Stable isotopes in tree rings - Toward a mechanistic understanding of isotope fractionation and mixing processes from the leaves to the wood. Tree Physiology doi:10.1093/treephys/tpu040.

Goldstein G, Andrade JL, Meinzer FC, Holbrook NM, Cavelier J, Jackson P, Celis A (1998) Stem water storage and diurnal patterns of water use in tropical forest canopy trees. Plant, Cell & Environment 21: 397–406.

Huang C, Domec J, Ward EJ, Duman T, Manoli G, Parolari AJ, Katul GG (2017) The effect of plant water storage on water fluxes within the coupled soil–plant system. New Phytologist 213: 1093–1106.

Hughes CE and Crawford J (2013) Spatial and temporal variation in precipitation isotopes in the Sydney Basin, Australia. Journal of Hydrology, 489: 42-55.

IPCC (2013) Climate Change 2013 – Impacts, Adaptation and Vulnerability Cambridge, In: Contribution of Working Group II to the Fourth Assessment Report of the IPCC (eds Parry M, Cantina O, Palutikof J, van der Linden P, Hanson C.), University Press, Cambridge United Kingdom.

James SA, Meinzer FC, Goldstein G, Woodruff D, Jones T, Restom T, Mejia M, Clearwater M, Campanello P (2003) Axial and radial water transport and internal water storage in tropical forest canopy trees. Oecologia 134: 37–45.

Kendall C, McDonnell JJ (1998) Isotope Tracers in Catchment Hydrology, Elsevier Sci. B.V., Amsterdam, 51–86.

Klein T, Zeppel MJB, Anderegg WRL, Bloemen J, De Kauwe MG, Hudson P, Ruehr NK, Powell TL, von Arx G, Nardini A (2018) Xylem embolism refilling and resilience against drought-induced mortality in woody plants: processes and trade-offs. Ecological Research 33: 839-855.

Knipfer T, Reyes C, Earles JM, Berry ZC, Johnson DM, Brodersen CR, McElrone AJ (2019) Spatiotemporal coupling of vessel cavitation and discharge of stored xylem water in a tree sapling. Plant Physiology 179: 1658–1668.

Konrad W, Katul G, Roth-Nebelsick A, Jensen KH (2019) Xylem functioning, dysfunction and repair: a physical perspective and implications for phloem transport. Tree Physiology 39: 243–261.

Kocher P, Horna V, Leuschner C (2013) Stem water storage in five coexisting temperate broadleaved tree species: significance, temporal dynamics and dependence on tree functional traits. Tree Physiology 33: 817–832.

Kuroda K, Yamane K, Itoh Y (2018) Cellular level in plant aanalysis of radial movement of artificially injected caesium in Cryptomeria japonica xylem. Trees 32:1505–1517.

Lehmann M, Goldsmith GR, Schmid L, Gessler A, Saurer M, Siegwolf RTW (2018) The effect of 18O-labelled water vapour on the oxygen isotope ratio of water and assimilates in plants at high humidity. New Phytologist 217: 105–116.

Logullo MA, Salleo S (1992) Water storage in the wood and xylem cavitation in 1-year-old twigs of Populus deltoides. Plant, Cell and Environment 15: 431–438.

Martinez-Vilalta J, Lloret F, Breshears DD (2012) Drought induced forest decline: causes, scope and implications. Biology letters, doi: 10.1098/rsbl.2011.1059.

Matheny AM, Bohrer G, Garrity SR, Morin TH, Howard CJ, Vogel CS (2015) Observations of stem water storage in trees of opposing hydraulic strategies. Ecosphere 6: 10.1890/ES15-00170.1

Meinzer FC, Brooks JR, Domec JC, Gartner BL, Warren JM, Woodruff DR, Bible K, Shaw C (2006) Dynamics of water transport and storage in conifers studied with deuterium and heat tracing techniques. Plant, Cell and Environment 29: 105–114.

Meinzer FC, Goldstein G, Andrade JL (2001) Regulation of water flux through tropical forest canopy trees: do universal rules apply? Tree Physiology 21: 19–26.

Mencuccini M, Salmon Y, Mitchell P, Hölttä T, Choat B, Meir P, O'Grady A, Tissue D, Zweifel R, Sevanto S, Pfautsh S (2017) An empirical method that separates irreversible stem radial growth from bark water content changes in trees: theory and case studies. Plant, Cell & Environment 40: 290–303.

Morris H, Plavcová L, Cvecko P, Fichtler E, Gillingham MAF, Martínez-Cabrera HI, McGlinn

DJ, Wheeler E, Zheng J, Ziemińska K (2016) A global analysis of parenchyma tissue fractions in secondary xylem of seed plants. New Phytologist 209: 1553–1565.

Nakada R, Okada N, Nakai T, Kuroda K, Nagai S (2019) Water potential gradient between sapwood and heartwood as a driving force in water accumulation in wetwood in conifers. Wood Scinece and Technology 53: 407–424.

Newberry SL, Nelson DB, Kahmen A (2017) Cryogenic vacuum artifacts do not affect plant water-uptake studies using stable isotope analysis. Ecohydrology https://doi.org/10.1002/eco.1892.

Orlowski N, Frede HG, Brüggemann N, Breuer L (2013) Validation and application of a cryogenic vacuum extraction system for soil and plant water extraction for isotope analysis. J. Sens. Sens. Syst. 2: 179–193.

Okada N, Hirakawa Y, Katayama Y (2011) Application of activable tracers to investigate radial movement of minerals in the stem of Japanese Cedar (Cryptomeria japonica). Journal of Wood Science 57: 421–428.

Okada N, Hirakawa Y, Katayama Y (2012) Radial movement of sapwood-injected rubidium into heartwood of Japanese cedar (Cryptomeria japonica) in the growing period. Journal of Wood Science 58: 1–8.

Penna D, Hopp L, Scandellari F, Allen ST, Benettin P, Beyer M, Geris J, Klaus J, Marshall JD, Schwendenmann L (2018) Ideas and perspectives: Tracing terrestrial ecosystem water fluxes using hydrogen and oxygen stable isotopes–challenges and opportunities from an interdisciplinary perspective. Biogeosciences 15: 6399–6415.

Peters RL, Fonti P, Frank DC, Poyatos R, Pappas C, Kahmen A, Carraro V, Prendin AL, Schneider L, Baltzer JL, Baron-Gafford GA, Dietrich L, Heinrich I, Minor RL, Sonnentag O, Matheny AM, Wightman MG, Steppe K (2018) Quantification of uncertainties in conifer sap flow measured with the thermal dissipation method. New Phytologist 219: 1283–1299.

Pfautsch S, Bleby TM, Rennenberg H, Adams MA (2010) Sap flow measurements reveal influence of temperature and stand structure on water use of *Eucalyptus regnans* forests. Forest Ecology and Management 259: 1190–1199.

Pfautsch S, Macfarlane C, Ebdon N, Meder R (2012) Assessing sapwood depth and wood properties in Eucalyptus and Corymbia spp. using visual methods and near infrared spectroscopy (NIR). Trees 26: 963-974.

Pfautsch S, Adams MA (2013) Water flux of *Eucalyptus regnans*: defying summer drought and a record heat wave in 2009. Oecologia 172: 317–326.

Pfautsch S, Renard J, Tjoelker MG, Salih A (2015a) Phloem as capacitor: Radial transfer of water into xylem of tree stems occurs via symplastic transport in ray parenchyma. Plant Physiology 167: 963–971.

Pfautsch S, Hölttä T, Mencuccini M (2015b) Hydraulic functioning of tree stems - fusing ray anatomy, radial transfer and capacitance. Tree Physiology 35: 706–722.

Pfautsch S, Harbusch M, Wesolowski A, Smith R, Macfarlane C, Tjoelker MG, Reich PB, Adams MA (2016) Climate determines vascular traits in the ecologically diverse genus *Eucalyptus*. Ecology Letters 19: 240–248.

Pfautsch, S (2016) Hydraulic anatomy and function of trees – basics and critical developments. Current Forestry Reports 2: 236–248.

Phillips NG, Ryan MG, Bond BJ, McDowell NG, Hinckley TM, Cermak J (2003) Reliance on stored water increases with tree size in three species in the Pacific Northwest. Tree Physiology 23: 237–245.

Rothfuss Y, Javaux M (2017) Reviews and syntheses: Isotopic approaches to quantify root water uptake: a review and comparison of methods. Biogeosciences 14: 2199.

R Core Team (2020) R: A language and environment for statistical computing. R Foundation for Statistical Computing, Vienna, Austria. https://www.R-project.org/.

RStudio Team (2020) RStudio: Integrated Development for R. RStudio, PBC, Boston, MA. http://www.rstudio.com/.

Sano Y, Okamura Y, Utsumi Y (2005) Visualizing water-conduction pathways of living trees: selection of dyes and tissue preparation methods. Tree Physiology 25: 269–275.

Secchi F, Pagliarani C, Zwieniecki MA (2017) The functional role of xylem parenchyma cells and aquaporins during recovery from severe water stress. Plant, Cell & Environment 40: 858–871.

Sevanto S, Hölttä T, Holbrook NM (2011) Effects of the hydraulic coupling between xylem and phloem on diurnal phloem diameter variation. Plant, Cell and Environment 34: 690–703.

Snyder RL, Shaw RH (1984) Converting Humidity Expressions with Computers and Calculators. Cooperative Extension, Leaflet 21372, Division of Agriculture and Natural Resources, University of California, Davis.

Sokołowska K, Zagórska-Marek B (2012) Symplasmic, long-distance transport in xylem and cambial regions in branches of Acer pseudoplatanus (Aceraceae) and Populus tremula 3 P. tremuloides (Salicaceae). American Journal of Botany 99: 1745–1755.

Thorburn PJ, Hatton TJ, Walker GR (1993) Combining measurements of transpiration and stable isotopes of water to determine groundwater discharge from forests. Journal of Hydrology 150: 563-587.

Vitvar T, Aggarwal PK, McDonnell JJ (2005) A review of Isotope Applications in Catchment Hydrology, in: Isotopes in the water cycle: past, present and future of a developing science. Eds: Aggarwal PK, Gat JR, Froehlich KF, Springer, The Netherlands, 151–169.

Volkmann THM, Kühnhammer K, Herbstritt B, Gessler A, Weiler M. 2016. A method for in situ monitoring of the isotope composition of tree xylem water using laser spectroscopy. Plant, Cell & Environment 39: 2055-2063.

Waring RH, Running SW (1978) Sapwood water storage: its contribution to transpiration and effect upon water conductance through the stems of old-growth Douglas-fir. Plant, Cell and Environment 1: 131–140.

Werner C, Schnyder H, Cuntz M, Keitel C, Zeeman MJ, Dawson TE, Badeck FW, Brugnoli E, Ghashghaie J, Grams TEE, Kayler ZE, Lakatos M, Lee X, Maguas´ C, Ogee´ J, Rascher KG, Siegwolf RTW, Unger S, Welker J, Wingate L, Gessler A (2012) Progress and challenges in using stable isotopes to trace plant carbon and water relations across scales. Biogeosciences 9: 3083–3111.

Walker CD, Richardson SB (1991) The use of stable isotopes of water in characterizing the source of water in vegetation. Chemical Geology 94: 145–158.

Wang A, Siegwolf RTW, Joseph J, Thomas FM, Werner W, Gessler A, Rigling A, Schaub M, Saurer M, Li M, Lehmann MM (2020) Effects of soil moisture, needle age and leaf morphology on carbon and oxygen uptake, incorporation and allocation: a dual labeling approach with 13CO2 and H218O in foliage of a coniferous forest. Tree Physiology: doi 10.1093/treephys/tpaa114.

Wershaw RL, Friedman I, Heller SJ, Frank PA (1966) Hydrogen isotopic fractionation of water passing through trees. Advances in Organic Geochemistry: 55.

Wheeler J, Huggett BA, Tofte AN, Rockwell FE, Holbrook NM (2013) Cutting xylem under tension or supersaturated with gas can generate PLC and the appearance of rapid recovery from embolism. Plant, Cell and Environment 36: 1938-1949.

White JWC, Cook ER, Lawrence JR, Broecker WS (1985) The D/H ratios of sap in trees - implications for water sources and tree-ring D/H ratios. Geochimica et Cosmochimica Acta 49: 237–246.

Wickham H (2016) ggplot2: Elegant Graphics for Data Analysis. Springer-Verlag New York.

Wullschleger SD, Hanson PJ, Todd DE (1996) Measuring stem water content in four deciduous hardwoods with a time-domain reflectometer. Tree Physiology 16: 809-815.

Zapater M, Hossann C, Bréda N, Bréchet C, Bonal D, Granier A (2011) Evidence of hydraulic lift in a young beech and oak mixed forest using 18O soil waterlabelling. Trees 25: 885–894.

Zhao L, Wang L, Cernusak LA, Liu X, Xiao H, Zhou M, Zhang S (2016) Significant difference in hydrogen isotope composition between xylem and tissue water in Populus euphratica. Plant, Cell & Environment 39: 1848–1857.

Zweifel R, Item H, Häsler R (2001) Link between diurnal stem radius changes and tree water relations. Tree Physiology 21: 869–877.

List of Figures

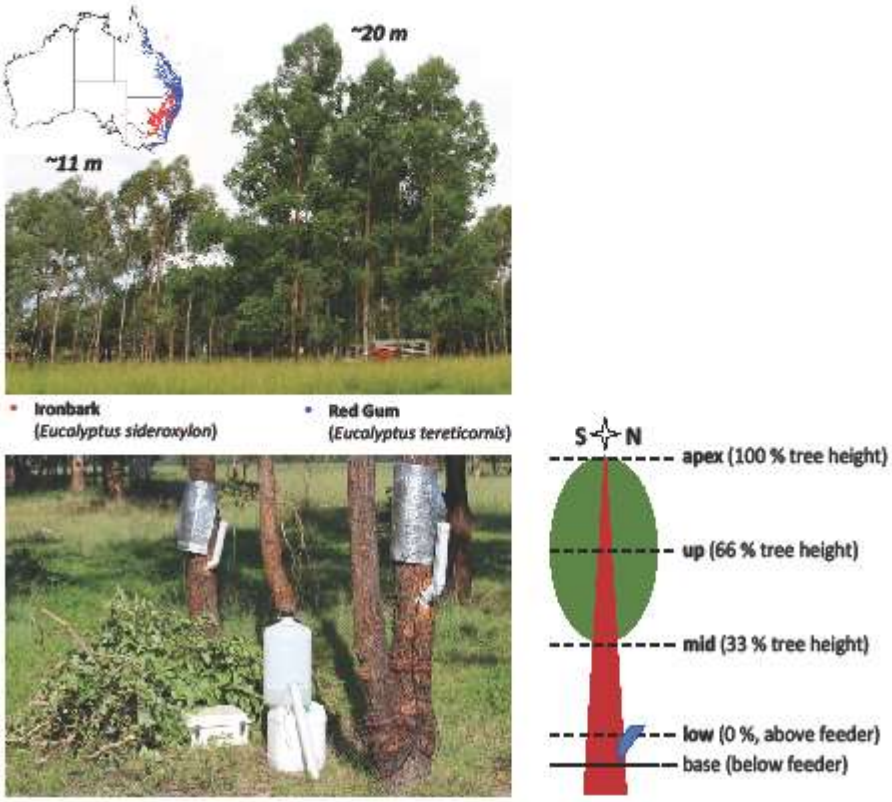

Figure 1: Study site and distribution of the two investigated species across Australia (upper picture). The map shows the natural ocurrence of Red Gum in blue and of Ironbark in red

(map source: https://avh.ala.org.au/). Installation of sapflow sensors (shielded) and water reservoirs at two out of three Ironbark trees (bottom picture) and scheme of sampling positions along each tree (right). The label strength of the injected δ^2H tracer was 1350 ‰.

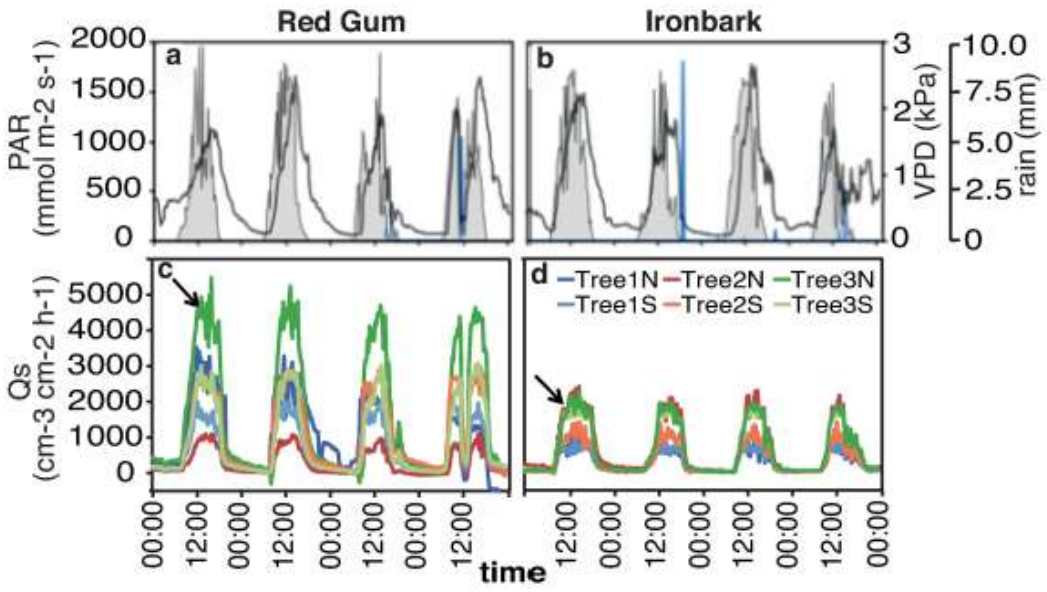

Figure 2: Diurnal variations of meteorological variables (a, b) and sapflow (c, d) of the three experimental trees of both species during the two study periods. Solid black lines in a and b represent vapor pressure deficit (VPD), grey shaded areas represent photosynthetically active radiation (PAR) and blue lines show rainfall events. c and d show sap flow density (Q_s) measured in the outer sapwood band at the northern (N) and southern (S) side of stems. Arrows indicate the time of installation of the water reservoirs containing the isotope tracer on the experimental trees (13 March 2014 in the morning on Red Gum and 20 March 2014 around noon on Ironbark).

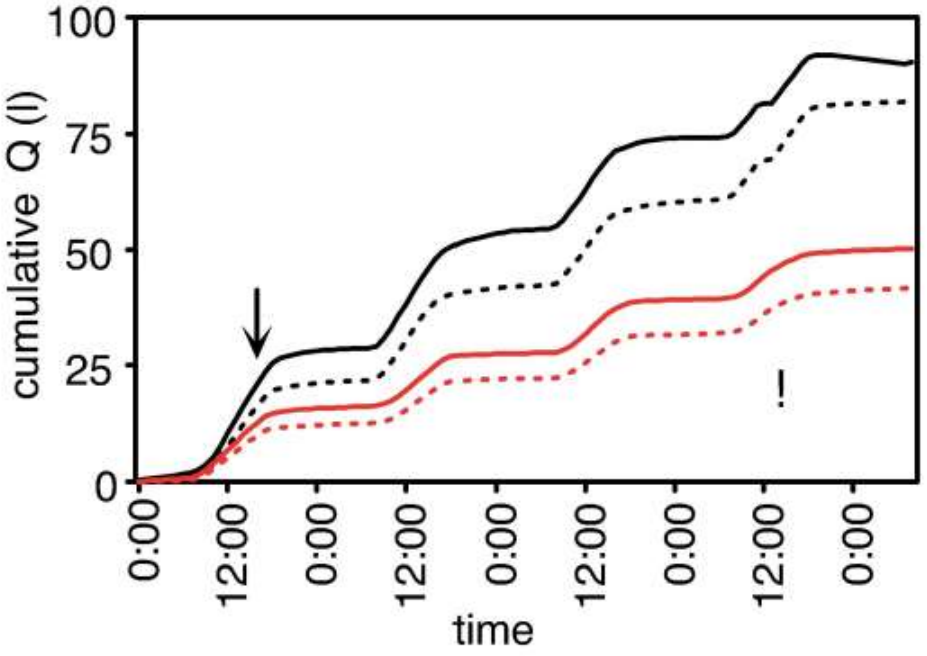

Figure 3: Average cumulative water use (*Q*) during four days of injection of deuteriated water into the northern side of three stems of Red Gum (black) and Ironbark (red). Water use was measured for the northern (solid line) and southern (dashed line) side of stems separately. The arrow indicates the start of tracer injection.

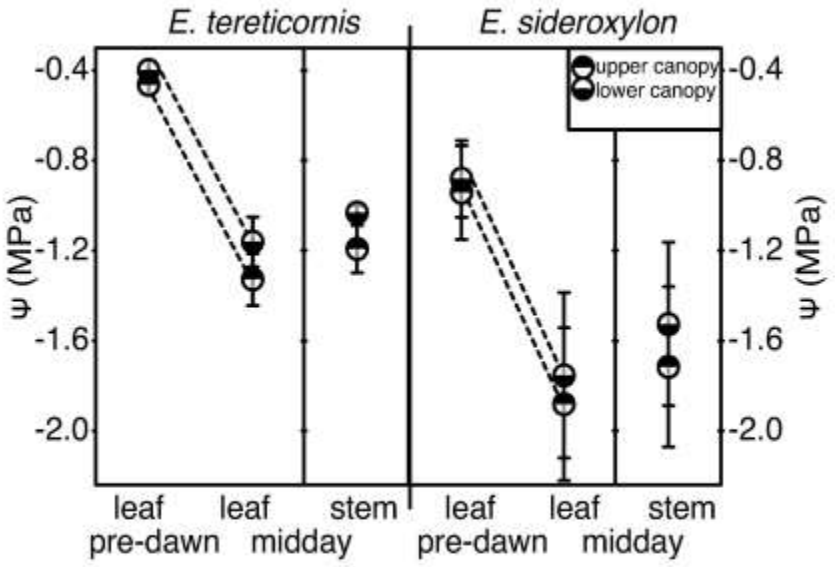

Figure 4: Pre-dawn and midday leaf water and stem water potentials. Measurements were conducted on 5 leaves per tree for leaf water potential and 3 leaves per tree for stem water potential (bagged leaves) both at the top of the canopy and the low canopy (n = 3 trees per species). Data shown are means of the individual measurements with their standard error.

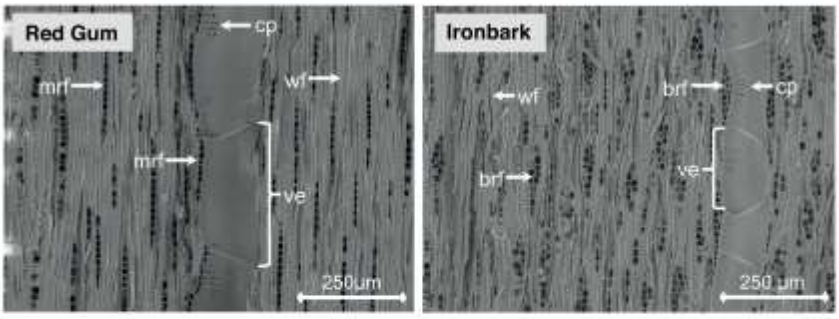

Figure 5: Electron microscope images of tangential sapwood sections of Red Gum and Ironbark. Clearly visible are vertical wood fibres (wf) and the broad bands of nonvestured contact pits (cp) connecting the vessels with ray cells. Individual vessel elements (ve) can also be seen. Arrangement of ray files and the abundance of individual rays strongly differ between Red Gum (monoseriate ray files (mrf), low ray abundance) and Ironbark (mostly biseriate ray files (brf), high ray abundance). Images were taken at 180X, low vacuum using 25kV acceleration voltage.

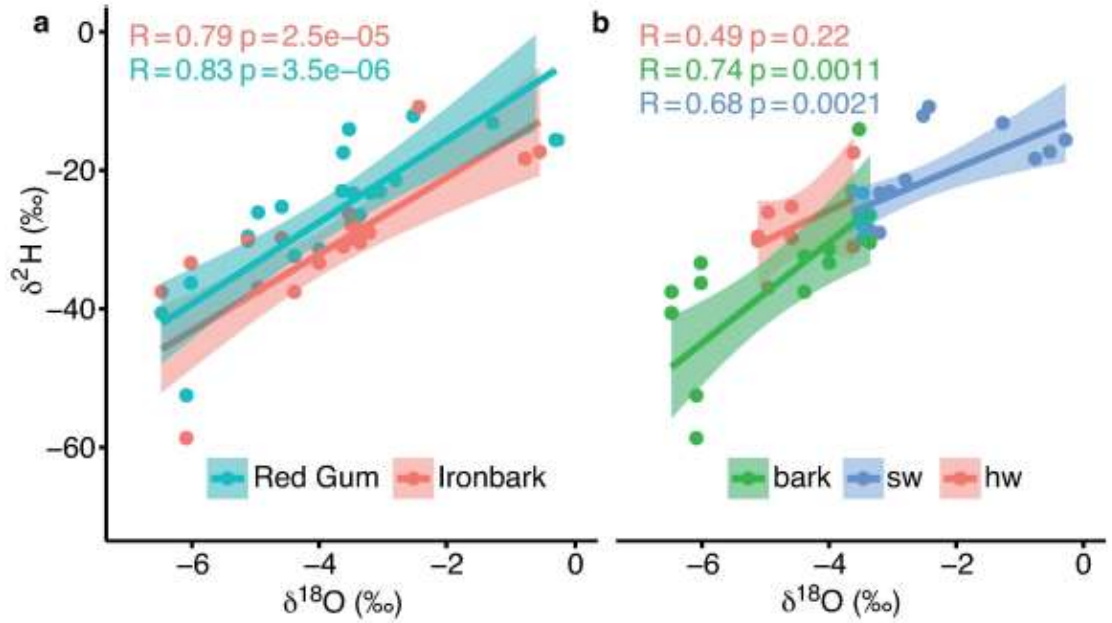

Figure 6: Distribution of δ^2H and $\delta^{18}O$ values at natural abundance and linear relationships between both, for all water samples of the control trees of both species (a) and separated in tissues (b). Notation 'bark' is inner bark water, 'sw' is sapwood water and 'hw' is heartwood water.

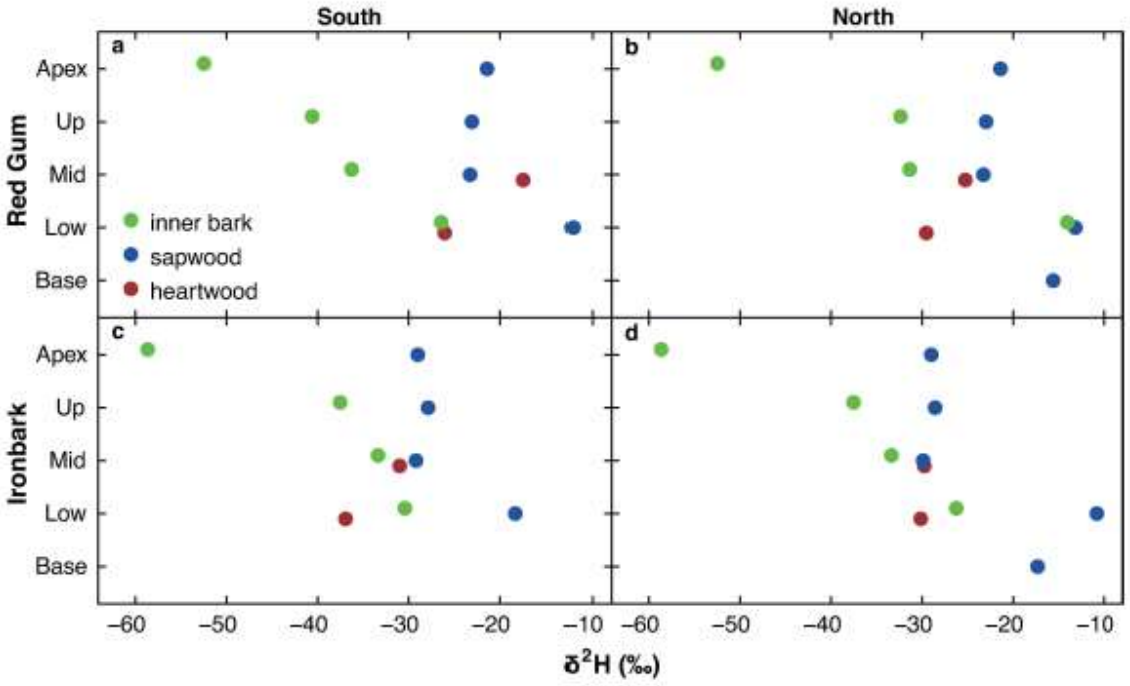

Figure 7: Distribution of δ^2H values at natural abundance in water of inner bark, sapwood and heartwood of the conrol tree of each species for all sampling positions in the stems.

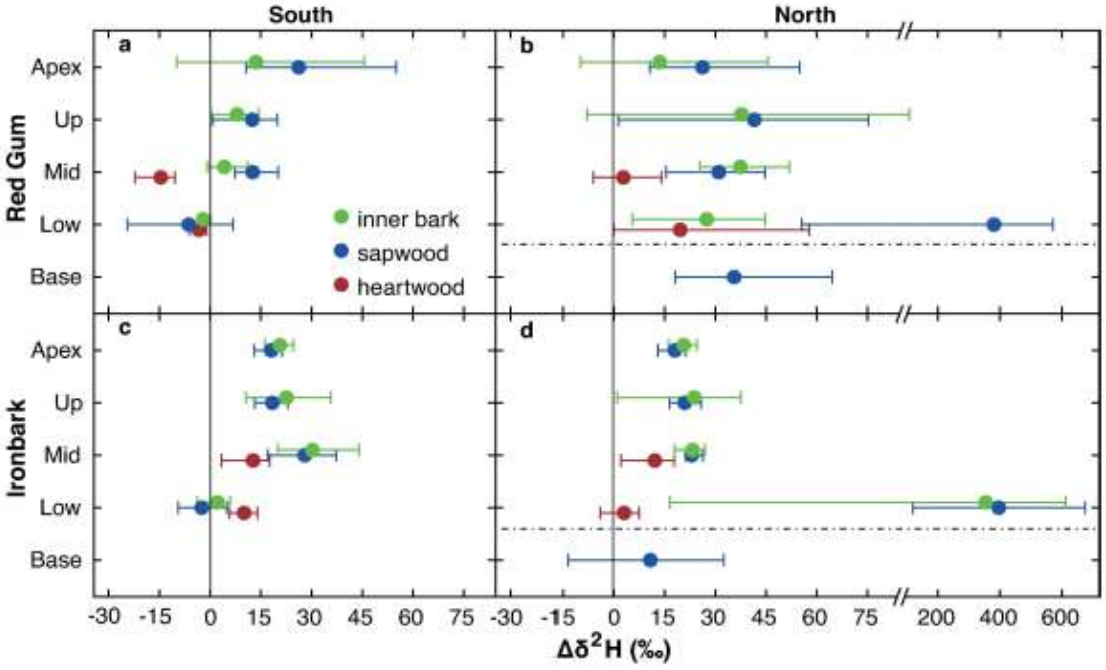

Figure 8: $\Delta\delta^2H$ deviations of the experimental trees from the controls for all sampling positions in the stems. Values above zero (vertical lines) indicate presence of the tracer in the corresponding sample. Dots are the means of the deviations of the three experimental trees and error bars indicate minimum and maximum values of the deviations from the control trees. Dotted lines in b and d indicate position of the water injection at the northern side of the stems.

Table 1: Moisture content (MC) in the tissues of three Red Gum (RG, n = 3) and Ironbark (IB, n = 3). Numbers in brackets indicate standard deviation. SW is sapwood and HW is heartwood.

Tree	Bark (%)	SW (%)	HW (%)
RG 1	59.87 (4.99)	47.54 (1.95)	53.85 (2.80)
RG 2	61.66 (1.09)	46.62 (1.67)	50.61 (4.66)
RG 3	63.37 1.60)	50.61 (2.29)	52.15 (1.48)
IB 1	47.58 (2.15)	38.39 (0.64)	37.19 (1.38)
IB 2	50.98 (7.90)	40.95 (1.81)	43.27 (2.09)

IB 3	51.21 (5.82)	63.73 (5.27)	30.72 (13.63)
Mean RG	**61.63 (2.56)**	**48.26 (1.97)**	**52.20 (2.98)**
Mean IB	**49.92 (5.29)**	**47.69 (2.57)**	**37.06 (5.70)**

Table 2: Stem characteristics of Red Gum and Ironbark trees used for sap flow measurements. Bark, sapwood and heartwood measurements were collected on the north and south facing sides of stems. Sapwood area was calculated using the mean values from both sides.

Species	Tree no.	Stem radius (mm)	Bark thickness north (mm)	Bark thickness south (mm)	Sapwod thickness north (mm)	Sapwod thickness south (mm)	Sapwood area (mm^2)	Heartwood thickness (mm)
Red Gum	1	165	17	17	28	27	22817	121
	2	110	13	15	25	33	14850	67
	3	138	12	12	43	36	26641	86
Ironbark	1	74	21	21	19	19	5551	37
	2	99	27	27	33	25	10386	43
	3	104	28	28	36	34	12865	41

Table 3: Anatomical characteristics of sapwood of Red Gum and Ironbark (n = 4 per species). Dv and D*h* are the vessel diameter and hydraulically weighted vessel diameter respectively. Numbers in brackets indicate standard deviation.

Species/ position		Stem height (m)	Stem diameter (cm)	Sapwood moisture content (%)	Sap-wood density ($g\ cm^{-3}$)	Mean Dv (µm)	Min Dv (µm)	Max Dv (µm)	D*h* (µm)	Vessel density (µm)	Void / wood ratio (%)
Red Gum	**Low**	1.22 (0.16)	25.50 (6.51)	48.67 (5.82)	0.58 (0.07)	151.69 (14.05)	31.30 (6.05)	243.74 (21.39)	193.27 (12.49)	446.17 (89.23)	9.20 (3.37)
	Mid	7.62 (1.22)	15.68 (4.15)	49.07 (2.33)	0.59 (0.04)	155.19 (27.75)	34.57 (7.07)	240.14 (42.31)	185.83 (31.76)	452.17 (37.55)	9.40 (3.11)
	Up	13.87 (2.06)	8.83 (1.47)	51.11 (2.20)	0.56 (0.04)	136.44 (34.77)	31.85 (6.83)	206.89 (35.09)	163.51 (33.64)	743.66 (405.66)	10.18 (1.86)
	Apex	20.24 (2.55)	0.50 (0.00)	NA	NA	31.99 (5.52)	9.85 (1.41)	65.15 (5.62)	47.68 (2.69)	12479.48 (3154.03)	11.18 (1.48)
Ironbark	**Low**	0.92 (0.33)	18.08 (2.47)	44.27 (2.01)	0.64 (0.02)	79.67 (6.23)	26.25 (0.78)	146.75 (12.28)	104.63 (6.20)	1431.98 (314.27)	8.17 (2.22)
	Mid	4.44 (0.52)	13.18 (1.32)	48.67 (1.24)	0.61 (0.02)	80.42 (6.33)	26.65 (1.16)	139.79 (5.62)	103.83 (3.66)	1620.70 (434.82)	9.02 (2.22)
	Up	7.67 (0.89)	6.08 (0.99)	49.03 (1.36)	0.59 (0.02)	76.44 (12.03)	26.18 (0.61)	135.76 (31.14)	93.23 (16.01)	2070.27 (269.20)	10.17 (2.43)
	Apex	11.17 (1.14)	0.50 (0.00)	NA	NA	17.56 (7.41)	6.21 (1.19)	36.34 (11.34)	26.76 (8.50)	56987.76 (11085.78)	10.35 (0.79)

Table 4: Anatomical characteristics of the wood rays in one *Red Gum* (RG) and one *Ironbark* (IB) tree. Numbers in brackets indicate standard deviation of cell counts of 10 images, each at three positions along the vertical stem axis (apex excluded as not enough material).

Position in the stem	number of rays	number of ray files	monoseriate rays (%)
RG 66 % tree height	654 (35.6)	77.46 (7.29)	93.73 (3.17)
RG 33 % tree height	596.87 (56.32)	71.15 (4.69)	97.64 (3.29)
RG 0 % tree height	717.79 (121.88)	80.96 (7.65)	76.9 (6.28)
IB 66 % tree height	669.77 (95.82)	127.23 (16.02)	72.19 (3.5)
IB 33 % tree height	647.69 (38.78)	111.8 (7.83)	65.39 (5.22)
IB 0 % tree height	806.81 (53.68)	120.22 (9.5)	64.17 (4.7)